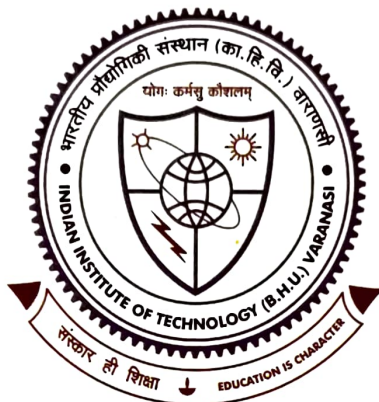


Synthesis and Characterizations of Substituted Ceramic Multiferroics



Thesis submitted in partial fulfillment for the
Award of the Degree
Doctor of Philosophy

By
Priyanka Verma

DEPARTMENT OF CERAMIC ENGINEERING
INDIAN INSTITUTE OF TECHNOLOGY
(BANARAS HINDU UNIVERSITY)
VARANASI - 221005
INDIA

Roll No.: 15031006

Year 2022

**Copyright ©
Department of Ceramic Engineering,
Indian Institute of Technology,
Banaras Hindu University, Varanasi-221005, India, 2022
All rights reserved.**

CERTIFICATE

It is certified that the work contained in the thesis titled "***Synthesis and Characterizations of Substituted Ceramic Multiferroics***" by "***Priyanka Verma***" has been carried out under my supervision and that this work has not been submitted elsewhere for a degree.

It is further certified that the student has fulfilled all the requirements of Comprehensive, Candidacy and SOTA.

Supervisor

(Associate Prof. P.K. Roy)
(Department of Ceramic Engineering)

Co-Supervisor

(Assistant Prof. Preetam Singh)
(Department of Ceramic Engineering)

DECLARATION BY THE CANDIDATE

I, "*Priyanka Verma*" certify that the work embodied in this thesis is my own bonafide work and carried out by me under the supervision of "*Dr. P.K. Roy*" from "*July 2015*" to "*July 2022*" at the "*Department of Ceramic Engineering, Indian Institute of Technology, Banaras Hindu University, Varanasi*". The matter embodied in this thesis has not been submitted for the award of any other degree/diploma. I declare that I have faithfully acknowledged and given credits to the research workers wherever their works have been cited in my work in this thesis. I further declare that I have not willfully copied any other's work, paragraphs, text, data, results, etc., reported in journals, books, magazines, reports, dissertations, thesis, etc., or available at websites and have not included them in this thesis and have not cited as my own work.

Date :

Signature of the Student

Place : Varanasi

(*"Priyanka Verma"*)

CERTIFICATE BY THE SUPERVISOR(S)

It is certified that the above statement made by the student is correct to the best of my knowledge.

Supervisor

Co-Supervisor

(*Associate Prof. P.K. Roy*)

(*Dr. Preetam Singh*)

(Department of Ceramic Engineering)

(Department of Ceramic Engineering)

Signature of Head of Department/Coordinator of School(s)

"SEAL OF THE DEPARTMENT/SCHOOL."

COPYRIGHT TRANSFER CERTIFICATE

Title of the Thesis: Synthesis and Characterizations of Substituted Ceramic Multiferroics

Name of the Student: Priyanka Verma

Copyright Transfer

The undersigned hereby assigns to the Indian Institute of Technology (Banaras Hindu University) Varanasi all rights under copyright that may exist in and for the above thesis submitted for the award of the “*Doctor of Philosophy.*”

Date:

Place: Varanasi

Signature of the Student

(Priyanka Verma)

Note: However, the author may reproduce or authorize others to reproduce material extracted verbatim from the thesis or derivative of the thesis for author's personal use provided that the source and the Institute's copyright notice are indicated.

ACKNOWLEDGEMENT

Life is a race and in today's fast-moving world, accomplishing a goal without the support of each other is a difficult task. Today, at the acme of my thesis, with heartiness, I gratefully remember many such individuals: as one flower makes no garland, this research would not have taken shape without their whole hearted encouragement and live involvement.

Foremost, I want to offer this endeavor to my *almighty Maa Santoshi* for the wisdom she bestowed upon me, the strength, peace of my mind and good health in order to finish my research. We all here are very thankful to *Madan Mohan Malaviya ji* co-founder of this institution.

I am highly indebted to my supervisor "*Dr. P.K. Roy*", Department of Ceramic Engineering, IIT (BHU), Varanasi, who inspires and encourage with his massive words and blessing, his unflinching support, constructive criticism, his truly scientific intuition and advice exceptionally inspired me and enriched my growth as a student. My involvement with his has triggered and nourishes my intellectual maturity that I will benefit for whole of my life.

With profoundest gratitude and great humility, I extend my gratefulness to my Co-Supervisor "*Dr. Preetam Singh*". He is a rare blend of scientific caliber and a person full of knowledge. He has been there all the time encouraging motivating and inspiring me.

I acknowledge with thanks the kind of patronage, loving inspiration and timely guidance, which I have received from my **RPEC members**, "*Prof. Ram Pyare*", (Internal subject expert) and "*Prof. Rajiv Prakash*" (External subject expert) School of material science and technology.

My sincere thanks to the Head “**Prof. Vinay Kumar Singh**” Department of Ceramic Engineering, IIT (BHU), Varanasi, for his kind support and for providing necessary lab facilities and a congenial working atmosphere in the Department.

I gratefully acknowledge central **instrumentation facility Centre (CIFC)**- IIT (BHU), Varanasi, for providing instrumental facilities through which I was able to perform my research smoothly and efficiently.

I also wish to thank all the **non-teaching staff** of the Department of Ceramic Engineering, Indian Institute of Technology (BHU) for their cooperation and timely help.

For me it is privilege to offer my overwhelming gratitude to my senior **Dr. Priyanka A. Jha and Dr. Pardeep Kumar Jha** for their intellectual vigor and generous support whenever needed. Their words have always fostered optimism and confidence in me.

My sincere thanks also go to my fellow lab mates **Mukesh Suthar, Akanksha Gupta**, for the stimulating discussions, for the times we were working together before deadline and for all the fun we have had during my research period.

This acknowledgement would not be complete without memorizing my **loving friends Dr. Shruti Singh, Somnath Mandal, Dr. Saddam Hossain**, for their invaluable help and co-operation during my stay in the campus. I really appreciate their ideas, help and good humor.

I can never forget to express deepest thanks to my life partner dear husband **Rakesh Verma** and my loving daughter **Dviti Birthaliya**. I would also express my eternal appreciation towards my **parents (Basant Kumar and Savitri Devi) and In-Laws (Ram Kumar and Sharda Devi)** who have always been there for me no matter where I am, for all the unconditional support and patience. Thank you for being so understanding and for never ending motivations I’ve been getting all this while.

Lastly, I owe my utterest gratitude to all the well-wishers **Shanti Devi, Ravi Kumar, Suman Verma, Sharija Kiroriwal, Pinki Prajapat, Amit Verma, Suman Verma, Jasit Verma, Mayank Prajapat, Himanshi Verma** who have willingly helped me out with their abilities in one way or the other.

Priyanka Verma

List of Figures

Fig. No.	Figure Caption	Page No.
Fig. 1.1	Classification of crystal classes	3
Fig. 1.2	Hysteresis loop for ferroic materials	4
Fig. 1.3	The perovskite structure	6
Fig. 1.4	Spin orientations of ferromagnetic, anti-ferromagnetics	8
Fig. 1.5	(a) A-type, (b) G-type, (c) C-type and (d) E-type commensurate antiferromagnetic order	10
Fig. 1.6	(a) sinusoidal and (b) cycloidal incommensurate antiferromagnetic order	10
Fig. 1.7	Different magnetic orders of superexchange interaction	11
Fig. 1.8	Classification of ferroic orders with symmetry	15
Fig. 1.9	(a) In BiFeO ₃ , (yellow) lobes of O ²⁻ ions and Bi ³⁺ (blue) ion contribute the polarization shown by red arrow, (b) Ferroelectricity due to inequivalent bonds, (c) Ferroelectricity due to inequivalent bonds.	16-17
Fig. 1.10	Simplified crystal structure of BiFeO ₃	18
Fig. 1.11	Phase diagram of BFO	20
Fig. 1.12	Ferroelectric hysteresis loop of BFO	21
Fig. 2.1	Different substituents shown in periodic table	24
Fig. 3.1	Sintering and calcination routes	46
Fig. 3.2	Flowchart of experimental procedure	47
Fig. 3.3	X-Rays production from an atom	49
Fig. 3.4	Principle of X-ray diffraction	50
Fig. 3.5	Working principle of FTIR.	54
Fig. 3.6	Principle of UV-Visible spectroscopy	55
Fig. 3.7	Principle of SEM	56
Fig. 3.8	EDS image of BFO	57
Fig. 3.9	Pellet used for Dielectric analysis	59
Fig. 3.10	Two-layer electric circuit diagram for Maxwell relaxation	61
Fig. 3.11	Sawyer-Tower electric circuit diagram for ferroelectric hysteresis loop measurement	63
Fig. 3.12	Working principle of MPMS	64
Fig. 3.13	Systematic diagram of XPS	65
Fig. 4.1	Tolerance factor of Bi _{0.9-x} Gd _x Sm _{0.1} FeO ₃ (x = 0.0, 0.025, 0.050, 0.075, 0.1)	68
Fig. 4.2	(a) XRD graphs of Bi _{0.9-x} Gd _x Sm _{0.1} FeO ₃ (x = 0.0 - 0.1), and (b) magnified pattern of peaks (104) and (110) at 2θ = 32° - 34°	69
Fig. 4.3	(a) Variation of lattice parameters with x, (b) Variation of Intensity I _{hkl} for peaks (104) and (110) with x, and (c)	70

	Variation of microstrain and Crystallite size for $\text{Bi}_{0.9-x}\text{Sm}_{0.1}\text{Gd}_x\text{FeO}_3$ ($x = 0.0 - 0.1$)	
Fig. 4.4	Relative density of pure BFO and Gd doped BSFO samples	71
Fig. 4.5	(a - e) SEM images using secondary electrons; and (f) Average grain size of $\text{Bi}_{0.9-x}\text{Gd}_x\text{Sm}_{0.1}\text{FeO}_3$ ($x = 0.0 - 0.1$)	72
Fig. 4.6	Grain size distribution curves of $\text{Bi}_{0.9-x}\text{Gd}_x\text{Sm}_{0.1}\text{FeO}_3$ ($x = 0.0-0.1$)	73
Fig. 4.7	Wavenumber vs. Transmittance of $\text{Bi}_{0.9-x}\text{Gd}_x\text{Sm}_{0.1}\text{FeO}_3$ ($x = 0.0 - 0.1$) samples	74
Fig. 4.8	Absorbance spectra of $\text{Bi}_{0.9-x}\text{Gd}_x\text{Sm}_{0.1}\text{FeO}_3$ ($x = 0.0, 0.025, 0.050, 0.075, 0.1$).	75
Fig. 4.9	Tau Tau _c 's plot of $\text{Bi}_{0.9-x}\text{Gd}_x\text{Sm}_{0.1}\text{FeO}_3$ ($x = 0.0, 0.025, 0.050, 0.075, 0.1$).	76
Fig. 4.10	Band gap variation with composition ($x = 0.0, 0.025, 0.050, 0.075, 0.1$).	77
Fig. 4.11	Dielectric constant variation with the Frequency at room temperature of samples $\text{Bi}_{0.9-x}\text{Gd}_x\text{Sm}_{0.1}\text{FeO}_3$ ($x = 0.0, 0.025, 0.050, 0.075, 0.1$).	77
Fig. 4.12	Dielectric loss variation with the Frequency at RT of samples $\text{Bi}_{0.9-x}\text{Gd}_x\text{Sm}_{0.1}\text{FeO}_3$ ($x = 0.0, 0.025, 0.050, 0.075, 0.1$)	79
Fig. 4.13	(a) Dielectric constant variation with temperature at 50 kHz Frequency; (b) Dielectric constant variation with temperature at 50 kHz Frequency for samples pure BFO and $\text{Bi}_{0.9-x}\text{Gd}_x\text{Sm}_{0.1}\text{FeO}_3$ ($x = 0.0, 0.025, 0.050, 0.075, 0.1$)	80
Fig. 4.14	Arrhenius conductivity plots for samples pure BFO and $\text{Bi}_{0.9-x}\text{Gd}_x\text{Sm}_{0.1}\text{FeO}_3$ ($x = 0.0, 0.025, 0.050, 0.075, 0.1$)	81
Fig. 4.15	M-H curves of BSFO samples; (b) Remanent magnetization variation with the substitution $\text{Bi}_{0.9-x}\text{Sm}_{0.1}\text{Gd}_x\text{FeO}_3$ ($x = 0.0, 0.025, 0.050, 0.075, 0.1$); and (c) Magnified image of $x = 0.0$, an anti-ferromagnetic nature of hysteresis loop.	83
Fig. 4.16	P-E loops of $\text{Bi}_{0.9-x}\text{Sm}_{0.1}\text{Gd}_x\text{FeO}_3$ ($x = 0.0, 0.025, 0.050, 0.075, 0.1$)	84
Fig. 5.1	Calculated variation of tolerance factor with composition of samples $\text{Bi}_{0.9}\text{Sm}_{0.1}\text{Fe}_{1-x}\text{Mg}_x\text{O}_3$ ($x = 0.0, 0.025, 0.050, 0.075, \text{ and } 0.1$)	87
Fig. 5.2	(a) XRD graphs of $\text{Bi}_{0.9}\text{Sm}_{0.1}\text{Fe}_{1-x}\text{Mg}_x\text{O}_3$ ($x = 0.0, 0.025, 0.050, 0.075, \text{ and } 0.1$); (b) Magnified pattern of peaks (110) and (104); (c) Magnified pattern of the secondary phase (Fe_2O_3)	89
Fig. 5.3	Rietveld refinement of $\text{Bi}_{0.9}\text{Sm}_{0.1}\text{Fe}_{1-x}\text{Mg}_x\text{O}_3$ series with $x = 0.0, 0.025, 0.050, \text{ and } 0.075$	90
Fig. 5.4	(a) Bond length (Fe-O) variation with the composition of $\text{Bi}_{0.9}\text{Sm}_{0.1}\text{Fe}_{1-x}\text{Mg}_x\text{O}_3$; $x = 0.0, 0.025, 0.050, \text{ and } 0.075,$	91

	(b) Crystal structure of pure BSFO sample in which different atoms are shown with different colors (red O-ions, green-Bi/Sm, inside of blue octahedra are Fe-ions)	
Fig. 5.5	FT-IR spectra of $\text{Bi}_{0.9}\text{Sm}_{0.1}\text{Fe}_{1-x}\text{Mg}_x\text{O}_3$ series with $x = 0.0, 0.025, 0.050, \text{ and } 0.075$	92
Fig. 5.6	BSE images of $\text{Bi}_{0.9}\text{Sm}_{0.1}\text{Fe}_{1-x}\text{Mg}_x\text{O}_3$ with $x = 0.0, 0.025, 0.050, \text{ and } 0.075$. Besides images show elemental mapping of sample with $x = 0.05$	94
Fig. 5.7	Average grain size variation with the composition.	95
Fig. 5.8	XPS complete survey of samples $\text{Bi}_{0.9}\text{Sm}_{0.1}\text{Fe}_{1-x}\text{Mg}_x\text{O}_3$ ($x = 0.0, 0.025, \text{ and } 0.075$)	96
Fig. 5.9	Gaussian fitted XPS spectra of Fe and O elements of samples $\text{Bi}_{0.9}\text{Sm}_{0.1}\text{Fe}_{1-x}\text{Mg}_x\text{O}_3$ ($x = 0.0, 0.025, 0.050, \text{ and } 0.075$)	97
Fig. 5.10	Gaussian fitted XPS spectra of Mg for samples $\text{Bi}_{0.9}\text{Sm}_{0.1}\text{Fe}_{1-x}\text{Mg}_x\text{O}_3$ ($x = 0.050 \text{ and } 0.075$)	99
Fig. 5.11	Hysteresis curves of samples of $\text{Bi}_{0.9}\text{Sm}_{0.1}\text{Fe}_{1-x}\text{Mg}_x\text{O}_3$ ($x = 0.0, 0.025, 0.050, \text{ and } 0.075$)	101
Fig. 5.12	ZFC curves of $\text{Bi}_{0.9}\text{Sm}_{0.1}\text{Fe}_{1-x}\text{Mg}_x\text{O}_3$ ($x = 0.0, 0.025, 0.050, \text{ and } 0.075$) fitted using logistic function.	103
Fig. 5.13	Brillouin behavior is explained by the fitted ZFC curve for Mg content $x = 0.05$	103
Fig. 5.14	M' vs M'' plots at temperature 370°C (643 K) of $\text{Bi}_{0.9}\text{Sm}_{0.1}\text{Fe}_{1-x}\text{Mg}_x\text{O}_3$ ($x = 0.0, 0.025, 0.050, \text{ and } 0.075$)	104
Fig. 5.15	M'' Vs. $\log(\nu)$ plot for $x = 0.05$. Inset shows the activation energy plot of the same	105
Fig. 5.16	(a) Current density variation with applied voltage of the samples of $\text{Bi}_{0.9}\text{Sm}_{0.1}\text{Fe}_{1-x}\text{Mg}_x\text{O}_3$ ($x = 0.0, 0.025, 0.050, \text{ and } 0.075$); (b) Average grain size variation with the composition	106
Fig. 5.17	$\ln J$ vs. $\ln E$ linearly fitted curves of the $\text{Bi}_{0.9}\text{Sm}_{0.1}\text{Fe}_{1-x}\text{Mg}_x\text{O}_3$ ($x = 0.0, 0.025, 0.050, \text{ and } 0.075$) samples	108
Fig. 6.1	Tolerance factor of $\{(1-x)(\text{Bi}_{0.9}\text{Sm}_{0.1})\text{FeO}_3 - (x)\text{Ba}(\text{Zr}_{0.15}\text{Ti}_{0.85})\text{O}_3\}$ (BSFO — BZT) ($x = 0.0, 0.1, 0.15, 0.2, 0.25, 0.5$) solid solution samples.	112
Fig. 6.2	X-ray Diffraction patterns of $(1-x)\text{Bi}_{0.9}\text{Sm}_{0.1}\text{FeO}_3 - (x)\text{BaZr}_{0.15}\text{Ti}_{0.85}\text{O}_3$ ($x = 0.0, 0.1, 0.15, 0.2, 0.25, 0.5$) samples	112
Fig. 6.3	Rietveld analysis of $(1-x)\text{Bi}_{0.9}\text{Sm}_{0.1}\text{FeO}_3 - (x)\text{BaZr}_{0.15}\text{Ti}_{0.85}\text{O}_3$ ($x = 0.0, 0.1, 0.15, 0.2, 0.25, 0.5$) samples	114
Fig. 6.4	Volume of $\{(1-x)(\text{Bi}_{0.9}\text{Sm}_{0.1})\text{FeO}_3 - (x)\text{Ba}(\text{Zr}_{0.15}\text{Ti}_{0.85})\text{O}_3\}$ (BSFO — BZT) ($x = 0.0, 0.1, 0.15, 0.2, 0.25, 0.5$) solid solution samples.	115

Fig. 6.5	SEM micrographs of (1-x) Bi _{0.9} Sm _{0.1} FeO ₃ — (x) BaZr _{0.15} Ti _{0.85} O ₃ (x = 0.0, 0.1, 0.15, 0.2, 0.25, 0.5) solid solution samples	115
Fig. 6.6	ϵ' , ϵ'' and $\tan\delta$ of (1-x) Bi _{0.9} Sm _{0.1} FeO ₃ — (x) BaZr _{0.15} Ti _{0.85} O ₃ (x = 0.0, 0.1, 0.15, 0.2, 0.25, 0.5) solid solution samples.	117
Fig. 6.7	Conductivity plots of (1-x) Bi _{0.9} Sm _{0.1} FeO ₃ — (x) BaZr _{0.15} Ti _{0.85} O ₃ (x = 0.0, 0.1, 0.15, 0.2, 0.25, 0.5) solid solution samples	119
Fig. 6.8	Activation energy calculated from real part of permittivity (ϵ') of (1-x) Bi _{0.9} Sm _{0.1} FeO ₃ — (x) BaZr _{0.15} Ti _{0.85} O ₃ (x = 0.0, 0.1, 0.15, 0.2, 0.25, and 0.5) solid solution samples.	121
Fig. 6.9	Conduction mechanism of (1-x) Bi _{0.9} Sm _{0.1} FeO ₃ — (x) BaZr _{0.15} Ti _{0.85} O ₃ (x = 0.0, 0.1, 0.15, 0.2, 0.25, 0.5) solid solution samples	123
Fig. 6.10	Z' vs. Frequency plot within different temperature region of (1-x) Bi _{0.9} Sm _{0.1} FeO ₃ — (x) BaZr _{0.15} Ti _{0.85} O ₃ (x = 0.0, 0.1, 0.15, 0.2, 0.25, 0.5) solid solution samples	125
Fig. 6.11	Z'' vs. Frequency plot within different temperature region of (1-x) Bi _{0.9} Sm _{0.1} FeO ₃ — (x) BaZr _{0.15} Ti _{0.85} O ₃ (x = 0.0, 0.1, 0.15, 0.2, 0.25, 0.5) solid solution samples	125
Fig. 6.12	Leakage current of (1-x) Bi _{0.9} Sm _{0.1} FeO ₃ — (x) BaZr _{0.15} Ti _{0.85} O ₃ (x = 0.0, 0.1, 0.15, 0.2, 0.25, 0.5) solid solution samples	126
Fig. 6.13	Schottky emission of (1-x) Bi _{0.9} Sm _{0.1} FeO ₃ — (x) BaZr _{0.15} Ti _{0.85} O ₃ (x = 0.0, 0.1, 0.15, 0.2, 0.25, 0.5) solid solution samples	127
Fig. 6.14	Space charge limited conduction of (1-x) Bi _{0.9} Sm _{0.1} FeO ₃ — (x) BaZr _{0.15} Ti _{0.85} O ₃ (x = 0.0, 0.1, 0.15, 0.2, 0.25, 0.5) solid solution samples	129

List of Tables

Table No.	Table Content	Page No.
Table 2.1	List of elements doped at Bi-site	25
Table 2.2	Effect of Sm doping on hexagonal and normalized unit cell parameters of BiFeO ₃	39
Table 2.3	List of results with Sm=0.1	40
Table 4.1	Force constant (<i>k</i>) and Bond length calculation of peaks in the range $\approx 538.21 - 549.27 \text{ cm}^{-1}$ of Bi _{0.9-x} Gd _x Sm _{0.1} FeO ₃ (<i>x</i> = 0.0, 0.025, 0.050, 0.075, 0.1)	74
Table 4.2	Room temperature dielectric constant (ϵ') and dissipation factor ($\tan\delta$) reported at frequency of 10.5 KHz for Bi _{0.9-x} Gd _x Sm _{0.1} Fe O ₃ (<i>x</i> = 0.0, 0.025, 0.050, 0.075, 0.1)	79
Table 5.1	Wavenumber, Effective mass, Force constant, Bond length calculated from FTIR; Bond angle and bond length calculated from Rietveld	93
Table 5.2	Findings from XPS data	99
Table 5.3	Fe content from EDX data	100
Table 5.4	Magnetic moment, temperature calculated from logistic equation	102

List of Symbols and Abbreviations

Notation	Abbreviations
<i>et al.</i>	et alia, Latin for “and others “
<i>i.e.</i>	That is
<i>e.g.</i>	Example
<i>etc.</i>	Et cetera, Latin for “and other similar things”
Fig.	Figure
UV	Ultra-violet
mg	Milligram
g	Gram
cm	Centimeter
Hz	Hertz
min	Minute
h	Hour
BFO	Bismuth ferrite
s^{-1}	Per Second
SCLC	Space charge limited conduction
<i>viz.</i>	Namely
IR	Infrared
XRD	X-ray diffractometer
SEM	Scanning electron microscopy
MPMS	Magnetic property measurement system
FESEM	Field emission scanning electron microscopy
MHz	Megahertz
RT or rt	Room temperature
EDX	Energy dispersive X-ray spectroscopy
SQUID	Superconducting quantum interference device
ZFC	Zero field cooled
FC	Field cooled
VSM	Vibrating sample magnetometer
P-E	Ferroelectric hysteresis loop
<i>MH</i>	Magnetic hysteresis loop
Approx..	Approximate
Equiv.	Equivalent
FWHM	Full width half maxima

M'	Real electrical modulus
M''	Imaginary electrical modulus
JCPDS	Joint Committee on Powder Diffraction Standards
XPS	X-ray Photoelectron Spectroscopy
R_F^2	(Structure R factor) ²
E	Applied Electric field
D	Average crystalline size
T_{irr}	Blocking or Irreversible temperature
R_b	Bragg factor
H_c	Coercive field
T_c	Curie temperature
FM	Ferromagnetic
J	Leakage current density
d_{33}	Piezoelectric coefficient
PVA	Polyvinyl Alcohol
P	Polarization vector
T	Temperature
H	Magnetic field
M	Magnetization
M_s	Saturation magnetization
H_c	Coercivity
M_r	Remanent magnetization
T_N	Ne'el temperature
γ^{obs}	Observed profile
γ^{cal}	Calculated profile
R_p	Profile residual factor
R_{wp}	Weight profile residual factor
R_{exp}	Expected profile residual factor
R	Resistance
C	Capacitance
a, b, c	Lattice parameters
j	Joule
J	Current density
E_a	Activation energy
K	Kelvin
i, j, k, l	spatial coordinates
k	kilo

Symboles used	
Symboles	Full name
α	Slope of curves
β	Full width half maxima
$^{\circ}\text{C}$	Degree Celsius
K	Kelvin
σ	Conductivity
©	Copyright
χ^2	Chi square
δ	Delta
>	Greater than
<	Less than
%	Percentage
Å	Angstrom
λ	Wavelength
&	And
π	Pi
±	Either plus or minus
\leq and \geq	Greater and Smaller- Than equal to
ω	Omega
χ	Magnetic susceptibility
μ_{eff}	Effective magnetic moment
ϵ	Dielectric permittivity
θ	Bragg's angle
μ_s	Spin magnetic moment
ν	wavenumber
I_e	Ionisation energy
K_B	Boltzmann constant
R_c	Richardson constant
c	Velocity of light
C	capacitance
ε	microstrain
∅	strain